Developing an efficient binding assay to quantify molecular interactions with the profilin protein.

By

Alexandra K. Hughson

Submitted to the Graduate Faculty of the

University Honors College in partial fulfillment

of the requirements for the degree of

Bachelor of Philosophy

University of Pittsburgh

2023

UNIVERSITY OF PITTSBURGH

UNIVERSITY HONORS COLLEGE

This thesis was presented by

by

Alexandra K. Hughson

It was defended on

March 16, 2023

and approved by

Dr. Zandrea Ambrose Ph.D., Associate Professor, Department of Microbiology and Molecular Genetics

Dr. David Koes Ph.D., Associate Professor, Department of Computational and Systems Biology

Dr. Mark MacBeth Ph.D., Associate Professor, Department of Chemistry and Biochemistry, Butler University

Thesis Advisor: Dr. Andrew VanDemark Ph.D., Associate Professor, Department of Biological Sciences

Developing an efficient binding assay to quantify molecular interactions with the profilin protein.

Alexandra K. Hughson, BPhil

University of Pittsburgh, 2023

After eye injuries, aberrant blood vessel growth, known as pathological ocular angiogenesis, can cause vision loss or blindness. This same pathological angiogenesis can also contribute to unregulated cell proliferation related to cancers. Previous research in animal models has shown that compounds that block actin-Pfn1 interactions can inhibit harmful angiogenesis. Native polyacrylamide gel electrophoresis (PAGE) offers an inexpensive, quick, and quantifiable assay system for screening interactions between Pfn1, actin, and anti-angiogenic C74 compounds. Unfortunately, wild type Pfn1 (WT-Pfn1) does not run into the gel on most native PAGE buffering systems since it has very little charge. To resolve this issue, a variant of profilin called profilin-3E (3E-Pfn1) was designed, adding three negatively charged residues to its N-terminus. 3E-Pfn1 is shown to be visualized on native PAGE, proving the viability of the assay. To prove the utility of 3E-Pfn1, it must be demonstrated that it functions biochemically and biophysically like WT-Pfn1. To do this, a protein thermal shift (PTS) assay is utilized to demonstrate that 3E-Pfn1 has a similar melting temperature to WT-Pfn1, and therefore would be biochemically similar. Likewise, structural modeling and crystallization techniques, previously employed on WT-Pfn1, are used to validate that 3E-Pfn1 is physically like that of the WT. In the future, native PAGE and PTS assays will be used to demonstrate that 3E-Pfn1 maintains polyproline binding as a further validation method. Once validated, 3E-Pfn1 can be utilized to quickly screen many future variants of C74 that are currently under development.

Table of Contents

Preface viii

1.0 Introduction 1

1.1 The Cytoskeleton 2

1.2 Actin 3

1.2.1 Angiogenesis 4

1.2.2 Actin Polymerization 5

1.3 Profilin 6

1.4 VEGF Pathway 7

1.5 Compound Development 8

1.5.1 *In Vitro* assay development with Native PAGE 11

1.5.2 Profilin Mutants 12

1.6 Objectives 14

1.7 Significance and Clinical Relevance 15

2.0 Methods 17

2.1 Cloning, Expression, and Protein Purification 17

2.2 Native PAGE 18

2.3 Crystallization 18

2.4 Protein Thermal Shift (PTS) Assay 19

2.5 Statistics 19

3.0 Results 20

3.1 Development of 3E-Pfn1 20

3.2 3E-Pfn1 completely moves into the native PAGE 23

3.3 3E-Pfn1 melting temperature shifts when proline peptide is added..... 27

3.4 Crystallization..... 29

3.5 Conditions for crystallization of 3E-PFN1 are determined..... 30

4.0 Discussion and Future Directions..... 32

References..... 36

List of Figures

Figure 1. Filaments of the cytoskeleton. **2**

Figure 2. Angiogenesis regulatory pathways. **7**

Figure 3. Structures of three iterations of anti-angiogenic compounds. **10**

Figure 4. Known binding domains on Pfn1. ..... **12**

Figure 5. Compound titration assay schematic on Native PAGE. **14**

Figure 6. Understanding the C74 drug complex. **15**

Figure 7. Cloning of 3E-Pfn1. ..... **20**

Figure 8. 3E-Pfn1 Purification on SDS PAGE. **21**

Figure 9. Sequence of "3E tag." **22**

Figure 10. 3E-Pfn1 runs favorably on native PAGE. **23**

Figure 11. Fluorescently labeled Ruby-3E-Pfn1 runs on native PAGE. **24**

Figure 12. High-Resolution Mass Spectrometry of 3E-Pfn1 ..... **25**

Figure 13. Conservation of WT-Pfn1 sequence among different species across evolution. **26**

Figure 14. Protein Thermal Shift Assay of 3E-Pfn1 and peptide. **27**

Figure 15. Hypothesized 3E-PFN1 structure. **29**

Figure 16. Crystallized WT-Pfn1 and 3E-Pfn1. ..... **30**

Preface

I would like to take this space to thank several of the people who helped and supported me throughout the research process and creation of this document. First and foremost, I would like to thank my advisor, Dr. Andrew VanDemark, for his unwavering support and guidance over the last two years. I truly could not have chosen a better mentor to help me carve out the beginnings of my research career. Additionally, I would like to thank the members of the VanDemark lab, specifically, Dr. Matthew Googins, Saeed Binsabaan, and Sara Zdancewicz for answering my never-ending questions and most importantly making my day-to-day lab experience enjoyable. I will always look back at my time in the VanDemark Lab with such appreciation and fond memories.

Additionally, I would like to thank the members of my committee: Dr. Zandrea Ambrose, Dr. David Koes, and Dr. Mark MacBeth for their time and feedback on this work. Likewise, I would like to thank the David C. Frederick Honors College for funding portions of this research and notably, Dr. Brett Say for inspiring me to take part in the BPhil process.

Lastly, and certainly not least, I would like to thank my family and friends. I thank my Dad and Mom, Chris and Susie Hughson, for always picking up the phone and grounding me with the best advice. I of course would also like to thank the ladies of 301 Coltart, for cheering me on these last four years. From Holland Hall to graduation soon, you all made my college experience so worthwhile.

1.0 Introduction

Angiogenesis is a critical cellular process necessary for the formation of new blood vessels from existing vasculature and is responsible for increased blood and nutrient flow (Qazi et al., 2009). In the body, angiogenesis is responsible for supplying blood to wounded areas and for generating vascularization through endothelial cells (ECs). However, when neovascularization becomes dysregulated, otherwise known as pathological angiogenesis, the new blood vessel growth can become functionally disruptive (Gau et al., 2018). As a result, when an event like a traumatic injury occurs in the eye, the new blood vessels formed by pathological angiogenesis may cause vision loss or blindness if they form over integral visual components (Qazi et al., 2009).

There are two pathways in which EC migration, and therefore angiogenesis, occurs. The pathway with the most clinical focus has been the vascular endothelial growth factor (VEGF) pathway. In patients with conditions characterized by pathological angiogenesis, anti-VEGF treatments are often used to target VEGF signaling to prevent further neovascularization and cancer cell growth (Allen et al., 2020). Unfortunately for many patients, the body can compensate for the absence of this signaling pathway, which can cause further cancer growth, despite the treatment (Gau et al., 2018). For this reason, the development of a new targeted therapy is necessary, and efforts have focused on targeting the interactions of two fundamental cytoskeletal proteins involved with other angiogenic pathway: actin and profilin.

1.1 The Cytoskeleton

The cytoskeleton is a critical part of eukaryotic cells that allows them to prevent damage, move and change shape, and transport intracellular molecules (Fletcher & Mullins, 2010). The main functions of the cytoskeleton in a eukaryotic cell can be grouped into three roles: specific organization of cell contents, biochemical and physical connections outside of the cell, and facilitation of cell movement and changes in shape (Fletcher & Mullins, 2010). The cytoskeleton is not a rigid structure, but rather is very dynamic, mobile, and made up of many different components and regulatory proteins (dos Remedios et al., 2003).

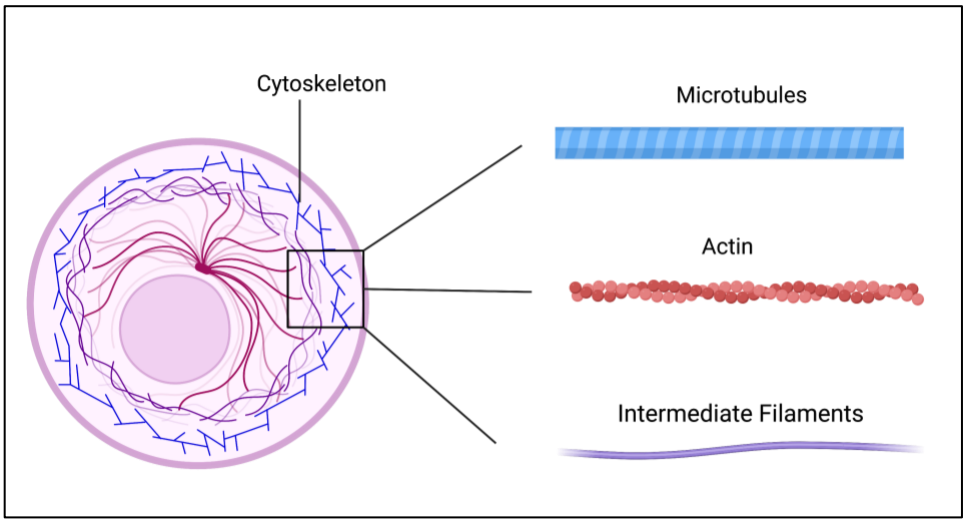

Figure 1. Filaments of the cytoskeleton.

The cytoskeleton is made up of microtubules, actin, and intermediate filaments. These filaments make up a rigid yet dynamic cytoskeleton that is important for cell growth and proliferation. Created with BioRender.com.

The cytoskeleton is made of filaments and tubules that possess the qualities that afford a cell the ability to be mobile and to differentiate in a very specific way (Figure 1). The

polymerization and depolymerization of filaments and microtubules control the mechanics of eukaryotic cells and respond to environmental stimuli (Fletcher & Mullins, 2010). These responses allow for the proliferation and migration of ECs, which are key components for capillary growth during angiogenesis (Ding et al., 2009). Cytoskeletal filaments made of actin as a main component, are further controlled by actin-binding regulatory proteins that help reinforce the assembly or breakdown of cytoskeletal structures (Fletcher & Mullins, 2010). Actin-binding regulatory proteins include the actin-sequestering proteins thymosin β4 and profilin; gelsolin, a barbed end capping protein; and capping antagonist vasodilator stimulated phosphoprotein (VASP); and many others. These proteins are key components in the regulation of the cytoskeleton and are integral for capillary morphogenesis, as well as cell remodeling and proliferation (Ding et al., 2009).

1.2 Actin

One protein that is an integral component of the cytoskeleton, is a filamentous protein called actin. Actin has a prominent regulatory role when it comes to cell dynamics, in which it controls cell shape and drives the organization of intracellular components (Fletcher & Mullins, 2010). Cells rely on actin within the cytoskeleton to divide via the rapid polymerization of actin monomers into actin filaments, followed by the construction of large filament networks, and then the breakdown of these filaments and networks back into monomers (Skruber et al., 2019). Actin provides the groundwork for maintaining cell morphology through adhesion, motility, exocytosis, endocytosis, and cell division (Rao & Li, 2004). For cells to continue dividing, they must always maintain a large supply of actin monomers.

The cell utilizes several regulatory components and a large pool of actin monomers, to render the cytoskeleton dynamic and allow it to quickly build and disassemble filaments. Actin is distributed throughout the cell and the cytoskeletal network by cell components, such as polymerases, monomer-binding proteins, and posttranslational modifications (Terman & Kashina, 2013). These posttranslational modifications are responsible for how actin is distributed throughout the cell and the cytoskeletal network (Terman & Kashina, 2013). It is well understood that in cells most actin monomers are bound to profilin, which has a crucial role in directing the growth of actin filaments within the cytoskeleton (Skruber et al., 2019). The tight regulation of actin dynamics is imperative, as dysregulation could lead to cancers and other negative phenotypes (Krüger et al., 2019).

1.2.1 Angiogenesis

Angiogenesis is the sprouting of new blood vessels from existing ECs, to facilitate cell growth and proliferation (Fierro, 2005). The role of angiogenesis is important for fundamental biological functions such as embryonic vascular development, organ regeneration, and wound healing (Ding et al., 2009). Angiogenic factors are membrane-bound stimulatory growth factors, which are responsible for the stimulation of angiogenesis during tissue repair and cell proliferation (Rafii et al., 2016). Angiogenic factors control the direction of the migration of ECs through the promotion of the budding of the capillary wall towards the angiogenic stimulus (Allen et al., 2020). Pfn1–actin interactions in ECs are a response to pro-angiogenic growth factors, which lead to signaling through a phosphorylation cascade involving phosphorylation of Tyr-129 on profilin (Gau et al., 2018). Angiogenesis is highly regulated by the vascular endothelial growth factor

(VEGF) pathway, which is specifically responsible for positively regulating the actin-Pfn1 interaction, and in turn leads to EC migration and proliferation (Gau et al., 2018). The phosphorylation-dependent mechanism described above has been proven both *in vitro* and *in vivo* through the blockage of the phosphorylation of Tyr129 on profilin. This phosphorylation hinders the interaction between Pfn1-actin, which causes a reduction in VEGF-induced cell motility through the reduction of angiogenesis (Gau et al., 2018). However, dysregulated angiogenesis, through dysfunction within the VEGF pathway, can lead to physiological issues like tumor growth and diabetic retinopathies from the neovascularization (Ding et al., 2009).

1.2.2 Actin Polymerization

The coordination of EC motility is highly regulated by actin and its role in angiogenesis. Within the cytoskeleton, actin is reorganized as part of EC migration and proliferation. Pfn1 enhances actin polymerization by catalyzing the ADP-to-ATP exchange on monomeric globular-actin or G-actin and transporting G-actin monomers to the barbed ends of actin filaments. Once Pfn1 becomes depleted, G-actin is reduced to filamentous actin or F-actin, completing the cycle of actin polymerization (Ding et al., 2009). Actin polymerization is integral to the formation of new cells via angiogenesis and is therefore tightly regulated by its interactions with proteins like Pfn1. However, there is now substantial evidence that changes in actin polymerization are a common occurrence in cancerous cells and that actin polymerization can be regulated by oncogenic signaling pathways (Rao & Li, 2004). This idea is key in cancers, like renal cell carcinoma which exhibits highly vascularized tumors due to loss of tumor-suppressing signaling that upregulates VEGF signaling and angiogenesis (Allen et al., 2020).

1.3 Profilin

Pfn1 is known to be both an actin polymerizing and sequestering molecule. Its role is to support actin polymerization by adding G-actin to the barbed end of actin filaments, creating F-actin (Ding et al., 2009). Due to its interaction with actin in the cytoskeleton, Pfn1 maintains a crucial role in angiogenesis and capillary morphogenesis within ECs (Ding et al., 2009). Pfn1 has a high affinity for proline-rich sequences and, in particular, those known to nucleate or elongate filamentous actin (Reinhard et al., 1995). Proline-rich domain protein families like VASP, are known to be essential mediators of cytoskeletal functions due to their interactions with Pfn1 (Reinhard et al., 1995). It has been shown that Pfn1 binding to polyproline-rich proteins enhances its binding affinity for actin, increasing the generation of F-actin (Ding et al., 2009). This interaction has been characterized and it is known that Pfn1 is upregulated during capillary formation from ECs (Allen et al., 2020). Specifically, vascular endothelial cells, or VECs, are a monolayer of ECs specific to the interior lining of arteries, veins, and capillaries. VECs have highly regulated cytoskeletal interactions and serve as ideal models for the study of Pfn1 interactions with actin (Krüger et al., 2019).

Pfn1 is also known to be a ligand for phosphatidylinositol-4,5- bisphosphate (PIP2). It is understood that the head group of PIP2 is able to remove actin monomers when bound to Pfn1 and to promote their assembly from G-actin into F-actin (Janmey et al., 2018). The binding site for PIP2 is near that of the actin binding site on Pfn1 (Lu & Pollard, 2001). As a result, PIP2 can decrease the affinity of the actin's binding to Pfn1 and allow actin to dissociate from Pfn1 more readily and enhances polymerization. The Pfn1 binding site on actin is near the site where actin binds to other monomers, therefore, Pfn1 must be removed before actin filaments can be formed

(Lu & Pollard, 2001). Understanding the role of Pfn1, and its protein regulators *in vivo* will inform the experimental design and anti-angiogenic compound development.

1.4 VEGF Pathway

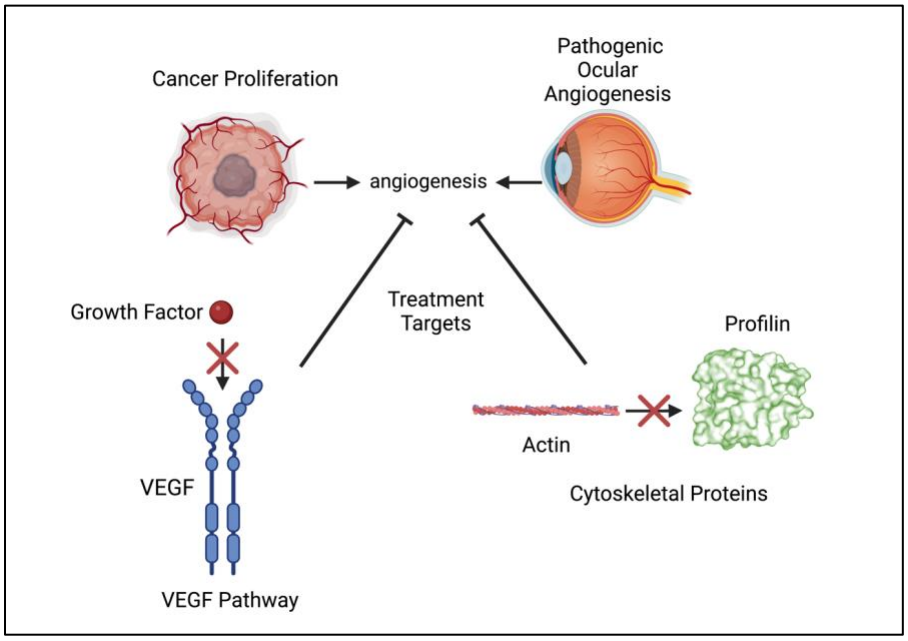

Figure 2. Angiogenesis regulatory pathways.

Although the VEGF pathway has been targeted to treat unwanted angiogenesis, it is not always effective. Alternative treatments are focused on disrupting the cytoskeleton directly through actin-profilin interactions. Created with BioRender.com.

The primary mechanism in which EC migration occurs via angiogenesis is through the VEGF pathway (Figure 2). VEGF is known to be the main growth signal involved in regulating the actin-Pfn1 interaction during angiogenic signaling of ECs (Allen et al., 2020). Through the VEGF pathway, phosphorylation of Pfn1 is induced in ECs, which is linked to positive regulation

of the Pfn1–actin interaction and pro-angiogenic factor production. When uncontrolled, the VEGF pathway can cause angiogenesis to be overactive, resulting in excessive neovascularization. When excessive angiogenesis occurs (i.e., pathological angiogenesis) rapid EC growth and proliferation can cause cancers or other disruptive pathologies (Allen et al., 2020). In addition to being an EC growth factor, VEGF is also an EC survival factor, which promotes angiogenesis through stimulation of cell proliferation and also inhibition of cell apoptosis (Fierro, 2005).

In patients with conditions characterized by pathological angiogenesis, anti-VEGF treatments are often used to target VEGF signaling. These targeted treatments prevent further cancer cell growth for cancers by eliminating the blood supply to the cells. However, in many cases, this treatment is effective initially, but after time, patients stop responding over time because an alternate pro-angiogenic pathway can become resistant to anti-VEGF treatment (Gau et al., 2018). These patients ultimately develop a progressive, drug-refractory disease. Therefore, research efforts are being directed toward molecules that are known to be fundamental for the regulation of angiogenesis and angiogenesis-related activities in ECs as an alternative method of treatment (Allen et al., 2020).

1.5 Compound Development

Previous work by our collaborators has identified compounds through structure-based virtual screenings. These compounds are designed to bind at the Pfn1-actin interface, and thus should block the ability of actin to recognize the binding site of Pfn1 (Gau et al., 2018). Through surface analysis using Pocket Query of Pfn1 (PBD code 2BTF), it was determined that Tyr169 and

Phe375 were the most important residues on actin for Pfn1 interaction (Ezezika et al., 2009). From the theorized Phe375 hydrophobic core, predicted pharmacophores were developed containing the essential structural features of the Pfn1-actin interaction (Gau et al., 2018). These were then utilized by Pharmer to search the ZINC database for existing compounds that could interact with the queried pharmacophores (Irwin et al., 2012). Compounds that scored well were then aligned to the pharmacophore and ranked based on properties, such as steric energy, to ensure the most optimal compound conformation. The two highest scoring compounds were identified as compound 1 (8-(3-hydroxyphenyl)-10-(4-methylphenyl)- 2,4,5,6,7,11,12-heptaazatricyclo[7.4.0.03,7]trideca-1(13),3,5, 9,11-pentaen-13-ol) and compound 2(8-(3-hydroxyphe-nyl)-10-phenyl-2,4,5,6,7,11,12-heptaazatricyclo[7.4.0.03,7]trideca1(13),3,5,9,11-pentaen-13-ol)), which were abbreviated to C1 and C2, respectively (Gau et al., 2018).

As stated previously, loss of function of Pfn1 leads to changes in the cytoskeleton, decreased cell migration, and proliferation of angiogenic VECs (Ding et al., 2009). To prove that C1 and C2 have the same cellular effects on angiogenesis as loss of Pfn1 function, a Matrigel cord formation assay with Hm-VEC-1 cells was performed. This assay is intended to show a dose-dependent decrease in the cord-forming ability in the cells when treated with compound. In this assay, the cord-forming ability of VECs can serve as a proxy for angiogenesis *in vivo.* The Matrigel cord formation assay has been used routinely as an *in vitro* morphogenetic assay to evaluate angiogenesis in endothelial cells (Gau et al., 2018). The results from these assays showed that C1 or C2 treated cells had a statistically significant decrease in cord-forming ability between controls when dosed between 50-100μM (Gau et al., 2018). However, the Matrigel cord formation assay cannot assess the sprouting ability of endothelial cells or represent the complexity of cellular interactions within multicellular organisms. For this reason, mouse aortic rings were analyzed

based on their endothelial cell sprouting ability before and after the addition of compound. Their findings were consistent with those from the Matrigel assay (Gau et al., 2018).

Although all assays performed have been initially promising in showing that C1 and C2 could have antiangiogenic effects, the concentrations needed to be effective therapeutically would be too high to be tolerated, as the compounds would become cytotoxic at 100µM (Gau et al., 2018). For this reason, further optimization of the compounds was necessary to increase binding affinity. To improve potency, additional docking calculations were performed for finding new related compounds, using the C2 compound as a scaffold (Allen et al., 2020).

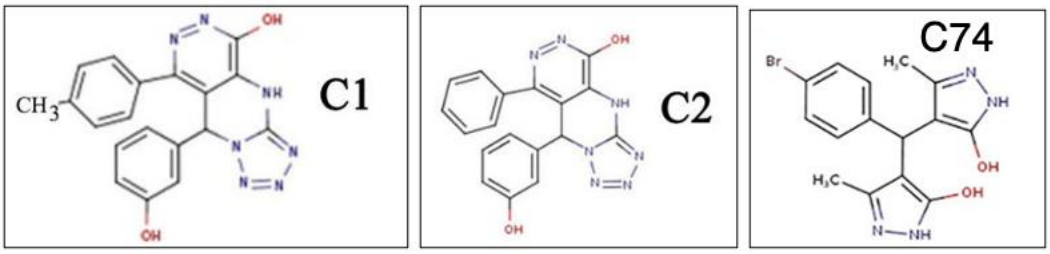

Figure 3. Structures of three iterations of anti-angiogenic compounds.

From computational screening and modeling, compounds C1 and C2 were identified as potentially having anti-angiogenic effects. After further optimization and screening, the C74 iteration of the compound was identified as being more effective *in vivo*.

From that screen, (4-[(4-bromophenyl) (5-hydroxy-3-methyl-1H- pyrazol-4-yl) methyl]-3-methyl-1H-pyrazol-5-ol) or C74 was identified as a unique compound that also decreased *in vitro* actin polymerization rates (Figure 3). C74 was shown to be functional *in vivo* to reduce angiogenesis and tumor growth in renal cell cancer cells at doses as low as 10µM, which was more therapeutically relevant than earlier iterations of the drug (Allen et al., 2020). This demonstrates

that C74 can be therapeutically effective and raises hopes that improved potency would allow it to be effective for pathological angiogenesis as well.

1.5.1 *In Vitro* assay development with Native PAGE

The primary *in vivo* assay used by our collaborators, is the Matrigel cord formation assay which is an effective *in vivo* screen. However, it is too slow and too costly to be an effective method for high throughput screening of compounds. For this reason, the development of a quick, efficient, and quantitative *in vitro* assay to screen many compounds rapidly is necessary to improve the speed of compound development and optimization. Thus, the native PAGE gel was selected as a possible method for drug screening, as it is known to separate proteins by charge and shape and has been utilized for many years to test protein-drug interactions (Wagstaff et al., 2005). The objective of the native PAGE assay was to test Pfn1-actin interactions and to quantify protein-drug interactions in one assay. This would allow the screening of many different compounds at once. However, WT-Pfn1 does not migrate well in native PAGE because of its minimal charge when using most traditional buffering systems which traditionally have a pH of about 8.8. With an isoelectric point (pI) of 8.49, Pfn1 moves towards the negative pole, which is off the top of the gel, preventing us from visualizing WT-Pfn1 by native PAGE. Previous efforts in the lab have tried different buffering systems or even reversing the electrodes, but none of these efforts offered solutions that would be practical and robust. For this reason, adjustments to the system were made through the development of a new variant of Pfn1, 3E-Pfn1, in which three negatively charged amino acids were added to the Pfn1 N-terminus to adjust the pI to 6.1.

1.5.2 Profilin Mutants

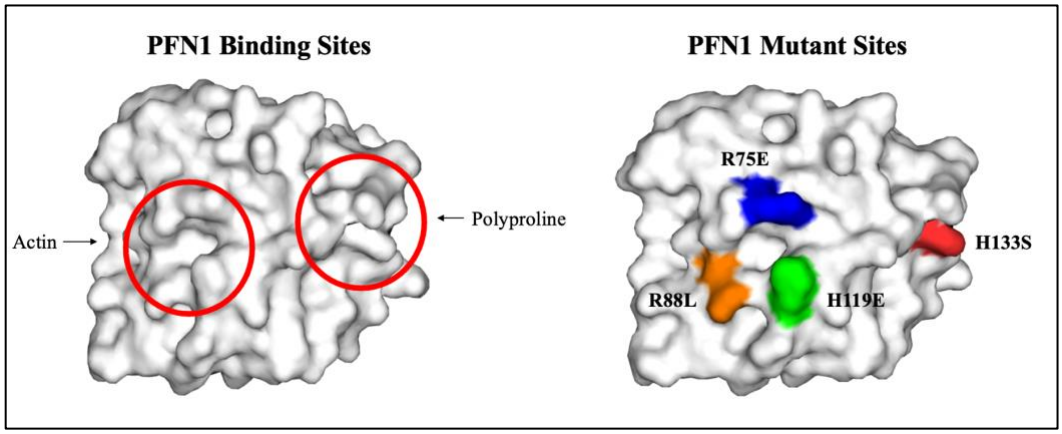

Figure 4. Known binding domains on Pfn1.

Pfn1 binding to actin is known to be regulated by its binding to polyproline motifs (Ding et al., 2009). The actin and polyproline binding pockets are labeled on the left. On the right, the four Pfn1 mutant residues are indicated. There are three mutations in the actin binding pocket and one in the polyproline binding pocket. Mutations at these sites are expected to either eliminate actin or polyproline binding and will function as binding controls on the native PAGE assay.

If 3E-Pfn1 is an appropriate surrogate for WT-Pfn1 in our binding assays, then it should mimic the binding behavior of WT-Pfn1, including binding all the binding partners that WT-Pfn1. Further, mutants that prevent these binding activities in WT-Pfn1 should do the same thing in the 3E-Pfn1 variant. For these purposes, I have generated four different mutations in the WT-Pfn1 and 3E-Pfn1 constructs as controls and means to test different binding interactions between Pfn1 and other cytoskeletal components (Figure 4). Additionally, these mutants will serve as binding controls to ensure that compounds are solely binding to Pfn1 or to determine if other mediating proteins are necessary for the interaction. In the H119E mutant, an important hydrogen bond to

Y169 of actin is lost which is believed to be the most critical interaction within the binding interface of actin and Pfn1 (Ding et al., 2009). Likewise, the H133S mutant has been shown to be defective in polyproline binding, an important mediator in the Pfn1-actin cytoskeletal complex (Ding et al., 2009). The R75E mutant disrupts PIP2 binding, which is relevant because the PIP2 binding site is known to overlap with the actin binding site (Ding et al., 2009). Lastly, the R88L mutant disrupts actin binding on the other side of the actin binding pocket on Pfn1 (Lu & Pollard, 2001). Together, these form a set of mutants that will investigate multiple important binding interactions of compounds to Pfn1.

The utilization of these mutants will be imperative in the development of an effective screening assay using native PAGE. It will be important to ensure that 3E-Pfn1 is functioning the same as that of the WT-Pfn1 protein, and these mutants will be useful controls for that purpose. Furthermore, it will be important to identify where a compound is binding to Pfn1 and what other protein mediators impact its binding. Through the disruption of binding through known mediators of the Pfn1-actin complex using the mutants above, it will be possible to rapidly determine the location and optimal conditions of compound binding, rapidly by native PAGE.

1.6 Objectives

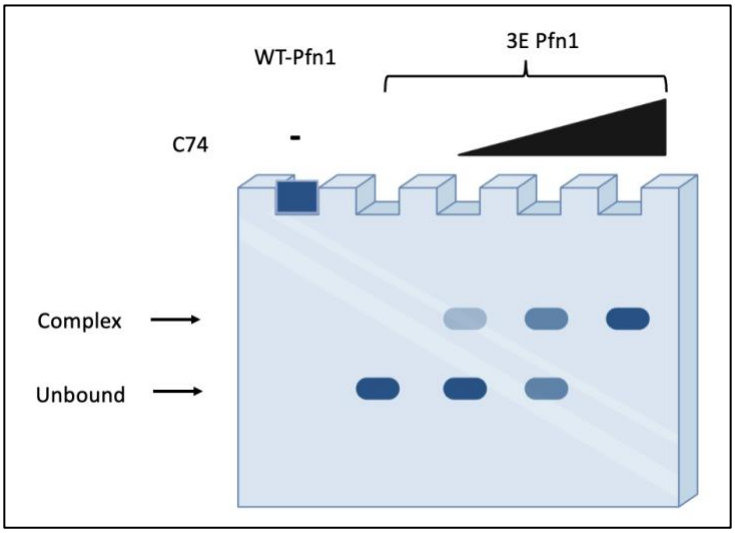

Figure 5. Compound titration assay schematic on Native PAGE.

As unbound 3E-Pfn1 binds to the ever-increasing amounts of C74 a slower migrating bound complex band begins to form and be visualized separately from unbound 3E-Pfn1 on Native PAGE. WT-Pfn1 cannot move into the gel due to its minimal charge and remains in the well. Created with BioRender.com.

My goal is to understand how C74 and other iterations of the compound disrupt the actin-Pfn1 binding interaction through the development of an *in vitro* native PAGE assay (Figure 5). This assay will allow for screening many compounds in a quick and inexpensive manner. From this assay, the derivation of a binding constant or K_D for Pfn1 and C74 can be derived. As a constant amount of 3E-Pfn1 is titrated with compound, a new band representing the 3E-Pfn1: Compound complex should be detected on the gel. The ratio of bound 3E-Pfn1 to unbound will be used to calculate the K_D. Having the binding interaction quantified in this way is important as a baseline for future improved iterations of the compound. Based on the existing cell-based data, it is anticipated that the K_D for this binding reaction could be as low as 25μM, but this interaction

has never been tested *in vitro* with purified reagents (Gau et al., 2018). The value measured will be the standard for comparison as we move forward with testing other derivatives of C74. Hopefully, they will be more potent and therefore have a lower K_D. Likewise, developing a complete assay with the appropriate controls as well as having a baseline will allow for quick screening of several improved compounds.

1.7 Significance and Clinical Relevance

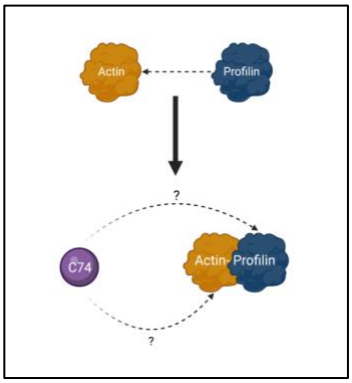

Figure 6. Understanding the C74 drug complex.

C74 disrupts the interaction between actin and profilin. Profilin binds to actin creating the actin-profilin complex. C74 is known to inhibit this through an undetermined mechanism. Created with BioRender.com.

Overall, understanding how C74 functions in disrupting actin-Pfn1 binding will provide a basis for the development and screening of future anti-angiogenic compounds (Figure 6). This goal is important because pathological ocular angiogenesis which occurs after an eye injury, is not

reversible, leading to permanent vision loss or blindness. Furthermore, these results can be generalized to other angiogenesis-mediated processes like the VEGF pathway and cancer proliferation, to hopefully develop alternative therapies for those who are resistant to anti-VEGF drugs. To accomplish this goal, the development or identification of new anti-angiogenic compounds with increased potency to be used as a therapy in the clinical setting is necessary. My research will institute the groundwork for an assay that will allow for quick identification of the best compounds, where our team can apply additional assays and techniques to characterize those interactions more thoroughly. This is an important aspect of the rationale drug-design process. In the future, this assay will be used to demonstrate improvements with C74-based therapeutic design, as our group plans to run the same analytical assays on improved iterations of the drug that are developed.

2.0 Methods

2.1 Cloning, Expression, and Protein Purification

The coding sequences for mouse PFN1 and all other constructs were PCR amplified and cloned into the pKF3 plasmid for bacterial protein expression fused with an N-terminal His10-mRuby2 tag, which can be removed through cleavage with Tobacco Etch Virus (TEV) protease. The resulting proteins retain GGS amino acids on their N-terminus. Expression was performed in BL21(DE3)-RIPL *E. coli* cells in lysogeny broth (LB) at room temperature by induction with 0.2 mM Isopropyl-ß-D-thiogalactopyranoside (IPTG) for 18-24 hours. Cells were then harvested and frozen at -80°C for at least 2 hours. Cells were then resuspended in 250mM NaCl, 10% Glycerol, 20mM Tris (2-carboxyethyl) phosphine (TCEP) pH 8, 5mM imidazole, 1µM 2-Mercaptoethanol (BME), and lysed by homogenization (Avestin C-3). Insoluble material was removed by centrifugation at 15,000 *x g* and His10-mRuby2-Pfn1 fusion protein captured using nickel affinity chromatography followed by digestion with TEV protease overnight to liberate Pfn1 protein from the His10-mRuby2 tag. A second round of nickel affinity chromatography was then performed to remove the tag and TEV. Finally, anion exchange chromatography and size exclusion chromatography were used to complete the purification. Protein quality was monitored throughout by SDS-PAGE.

2.2 Native PAGE

Analysis of protein-protein interactions was conducted through PAGE. This is conducted by mixing potential ligands with 3E-Pfn1 protein at a final concentration of 30 μM. The reaction buffer was 50mM Tris pH 8, 5mM NaCl, and 1μM BME and incubation was performed for 30 minutes on ice. Reactions were loaded using 4x Native loading buffer [200 mM Tris pH 6.8, 50% glycerol] and run on 10% PAGE for 3.5 hours at 180 volts. Gels with fluorescently labeled protein were imaged using an Amersham Imager 600 (General Electric) on the epi-luminescence setting. Afterward and in all other cases, gels were stained with Coomassie stain and imaged using an Amersham Imager 600 (General Electric) transillumination setting.

2.3 Crystallization

3E-Pfn1 was purified as described above and stored at 4°C prior to crystallization. Crystals were grown using sitting-drop vapor diffusion method at 4°C. One μL of protein at 13 mg/mL was added to 1 μL of well solution containing 1.85 M ammonium sulfate and 0.1M citric acid, pH 3.9. The original protein was at a concentration of 7.5 mg/mL in a buffer of 50mM HEPES pH 8, 5mM NaCl and 1μM BME. Small rectangular crystals grew over the course of 2-3 weeks.

2.4 Protein Thermal Shift (PTS) Assay

PTS experiments were carried out in 20uL volume in triplicate, with each sample containing 3E-Pfn1 at 0.3mg/mL concentration in optimized PTS buffer (50mM HEPES pH 8, 30mM NaCl, 5% glycerol, 1mM β-ME), with GloMelt dye at 0.4X concentration and the passive reporter ROX dye at 50nM concentration (33022-1, Biotium). Samples were added to a 96-well plate compatible with the QuantStudio™ 3 Real-Time PCR System (A28567 ThermoFisher) and then underwent denaturation using a temperature gradient that increased from 30˚C to 90˚C at a rate of 0.05˚C per second. Fluorescent intensity at each step was recorded and was analyzed by plotting the fluorescent intensity derivative as a function of temperature to generate a melt curve for each sample. 3E-Pfn1 was tested in the presence of polyproline peptide as well as a buffer vehicle control of 1% Triton and 25mM Tris pH 8. The melting temperatures for the triplicates of each dilution point were averaged to determine Tm for each concentration point. The absolute value of the change in Tm was taken and plotted as a function of compound concentration to generate a binding curve for 3E-Pfn1 and the peptide. Although Tris is not typically used in PTS assays because it is thermo-sensitive, the peptide was already in a buffer containing Tris prior to this experiment, so this was accounted for within the buffer vehicle control.

2.5 Statistics

The Wilcoxon-Mann-Whitney test was used to assess the significance of melting temperature shifts between protein and protein complexes ($p<0.05$).

3.0 Results

3.1 Development of 3E-Pfn1

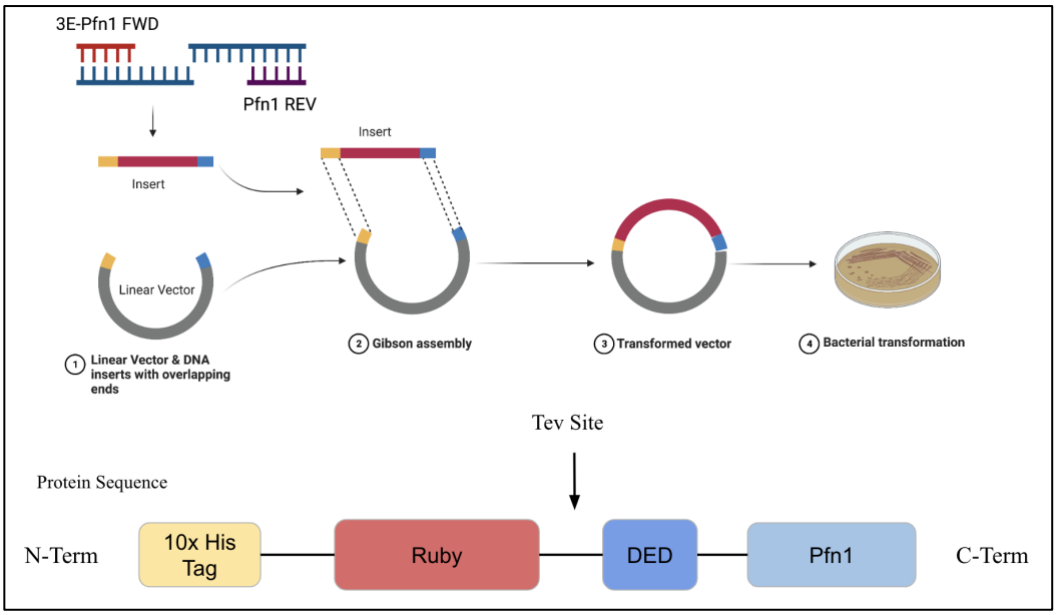

Figure 7. Cloning of 3E-Pfn1.

3E-Pfn1 was cloned using a known Pfn1 reverse primer and a novel 3E-Pfn1 forward primer to add the three amino to the insert. The insert was then added into the pKF3 plasmid through Gibson assembly. Shown at the bottom is the resulting 3E-Pfn1 protein sequence which was optimal for protein purification.

WT-Pfn1 has a PI of 8.49 rendering it with nearly no charge at the pH of electrophoresis, and therefore unable to move towards the positively charged electrode at the bottom of the native PAGE gel. To make Pfn1 better suited for native PAGE, I made a new variant of Pfn1, 3E-Pfn1, in which I have added three negatively charged amino acids to the Pfn1 N-terminus by polymerase chain reaction using a known reverse WT-Pfn1 primer and a newly developed 3E-

Pfn1 forward primer, which was then cloned into the pKF3 plasmid (Figure 7). 3E-Pfn1 has an aspartic acid, followed by a glutamic acid, then another aspartic acid at the N-terminus but was coined 3E-Pfn1 for short because DED-Pfn1 seemed too pessimistic. With these additional amino acids, 3E-Pfn1 has an overall net negative charge and PI of 6.11, which we hypothesized would allow it to migrate into the native PAGE towards the positively charged pole. 3E-Pfn1 was cloned into the His-mRuby2 vector (Figure 7), where the histidine residues and ruby tag could be exploited for purification via nickel-affinity chromatography (Figure 8).

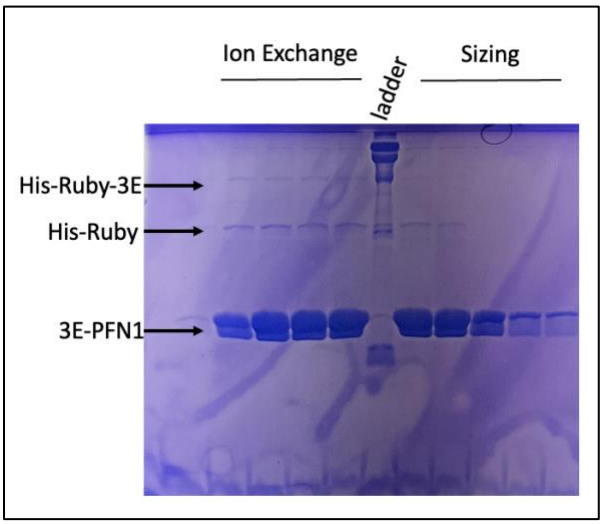

Figure 8. 3E-Pfn1 Purification on SDS PAGE.

3E-Pfn1 was purified through nickel affinity chromatography, anion exchange chromatography, and size exclusion chromatography. After the final step, samples were free of contaminants and fusion products. Sizing lanes 1-3 were collected with an average protein concentration of 5.3 mg/mL.

I cloned four mutants of Pfn1, H119E, H133S, R88L, and R75E, into the "3E" backbone, so that they could be visualized on native PAGE (Figure 9). Following this step, 3E-

Pfn1 and the four mutants were expressed, purified, and run on SDS PAGE to confirm that each sample was pure and different in molecular weight than WT-Pfn1.

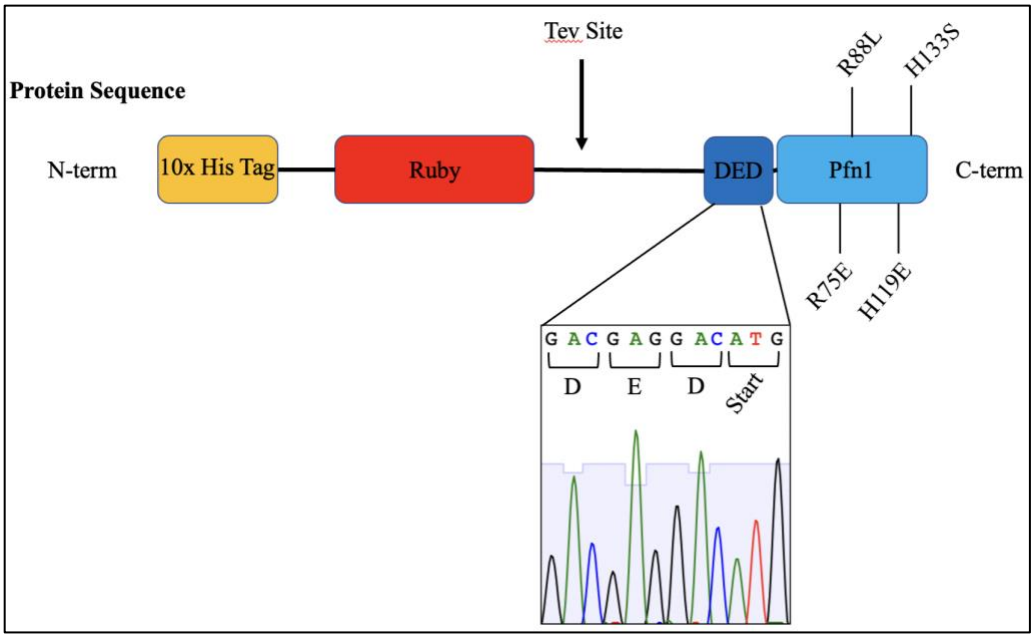

Figure 9. Sequence of "3E tag."

Wildtype and mutant Pfn1 constructs were tagged at their N-termini with an aspartic acid, glutamic acid, followed by another aspartic acid. The Pfn1 methionine start codon immediately follows. The success of the DED or "3E" tag addition was confirmed by sequencing as can be seen in the graph.

3.2 3E-Pfn1 completely moves into the native PAGE

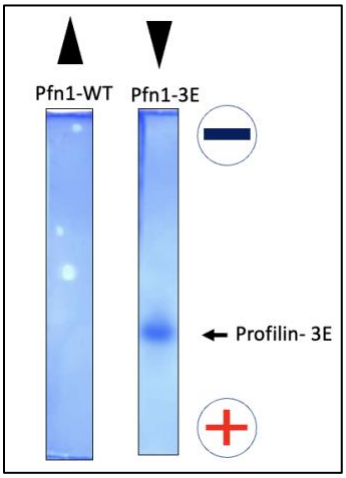

Figure 10. 3E-Pfn1 runs favorably on native PAGE.

Native PAGE of Pfn1 variants. Migration of WT-Pfn1 and 3E-Pfn1 on 10% native PAGE using standard buffering conditions. WT-Pfn1 runs off the top of the gel towards the negative electrode as 3E-Pfn1 runs into the gel towards the positive electrode. 3 mg/mL of each protein was loaded onto the gel. Created with BioRender.com.

After cloning, expressing, and purifying the 3E-Pfn1 protein, I then tested its migrations on a native PAGE gel. To do so, I took purified samples of WT-Pfn1 or 3E-Pfn1 and ran equal amounts of each from stocks at 30µM on the native PAGE. A total of 3 mg/mL was run for each sample. The gel was a 10% native PAGE and ran at 180 volts for two hours and twenty minutes, after which it was stained with Coomassie. From this experiment, I observed that 3E-Pfn1 ran into the native PAGE while WT-Pfn1 did not (Figure 10). This confirmed that the addition of the three negatively charged residues gave 3E-Pfn1 the ability to run on native PAGE.

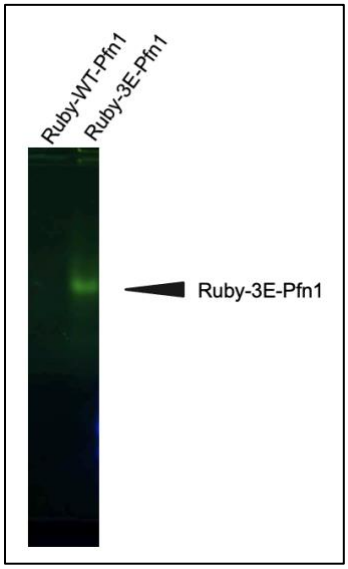

Figure 11. Fluorescently labeled Ruby-3E-Pfn1 runs on native PAGE.

mRuby2-tagged 3E-Pfn1 runs on 10% native PAGE. mRuby2-WT-Pfn1 was also run on native PAGE as a control but could still not be visualized due to its minimal charge.

Likewise, I determined whether 3E-Pfn1 fluorescently tagged with His-mRuby2 would also be visualized on native PAGE gel. This would be advantageous as any assays run to test binding interactions could be analyzed via fluorescence and therefore allow me to calculate a K_D for the binding interaction in another way. I was able to see both mRuby2-tagged 3E-Pfn1 sufficiently on the gel (Figure 11). This assay will be the basis for future native PAGE assays, as it could be used to quantify binding interactions and calculate a K_D fluorescently.

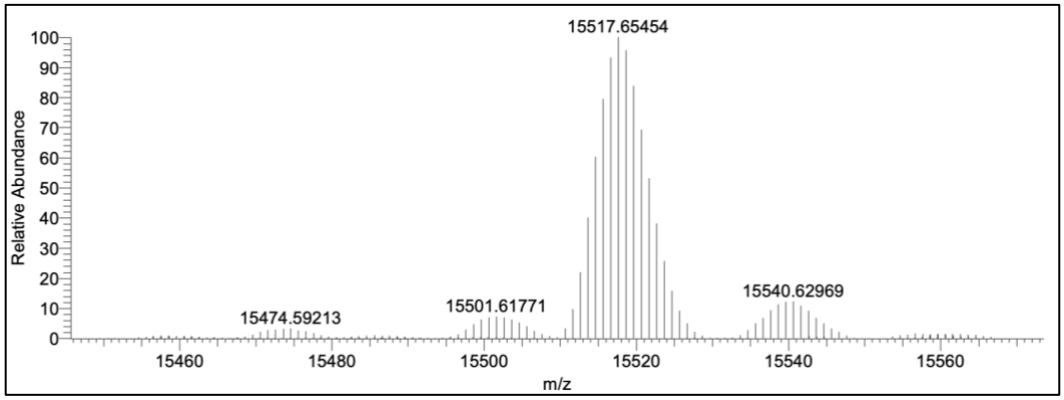

Figure 12. High-Resolution Mass Spectrometry of 3E-Pfn1.

Mass spectrometry peak was performed of 3E-Pfn1 with a denoted mass of 15,517.65 Daltons. The peak on the left with a mass of 15,501.62 Daltons likely indicates the loss of an oxygen. The peak on the right with a mass of 15,540.63 Daltons likely indicates the addition of a sodium ion to the protein.

To confirm that 3E-Pfn1 had the DED tag added to Pfn1 N-terminus, mass spectrometry was performed. Mass spectrometry can accurately calculate the molecular weight of a protein out to four decimal places through analysis of the mass-to-charge ratio of the protein (Brenton & Godfrey, 2010). This is a precise way to determine that the appropriate residues are present after the protein purification process. The molecular weight of WT-Pfn1 without the three added residues is 15,158.6 Daltons and the molecular weight of 3E-Pfn1 was expected to be 15,517.4 which was confirmed in our sample (Figure 12). It should be noted that three residues (GGS) remain at the N-terminus after cleavage with TEV.

From the resulting mass spectrometry data, the main peak of 15,517.65 Daltons was nearly the exact expected molecular weight for 3E-Pfn1, and therefore confirmed that the protein was successfully cloned and purified with the three added residues to WT-Pfn1. There were two other peaks to the left and right of the main 3E-Pfn1 peak. The small peak on the left with a molecular weight of 15501.62 Daltons likely resulted from either a contaminant or decarboxylation of the

3E-Pfn1 protein. The other peak with a molecular weight of 15,540.63 Daltons likely resulted from the presence of a sodium ion, which can sometimes be retained with the protein as it goes through the mass spectrometer. The addition of the sodium ion is likely due to high salt concentrations in the buffer used for the experiment. Regardless, these peaks are insignificant compared to the predominant peak and do not represent any significant amino acid changes that would impact the morphology of the protein.

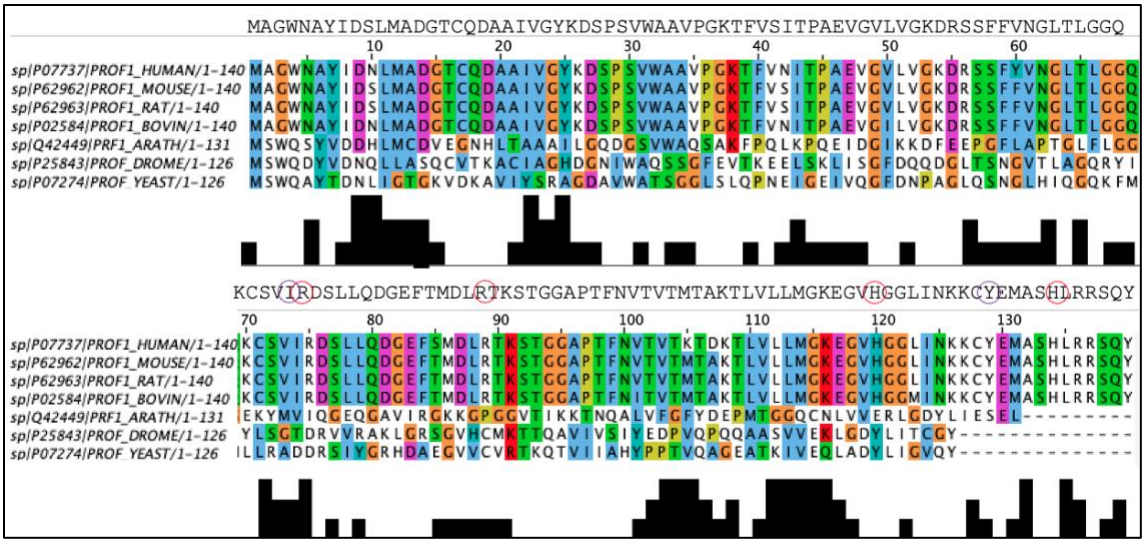

Figure 13. Conservation of WT-Pfn1 sequence among different species across evolution.

The sequence of Pfn1 is well conserved across species over evolution. The mouse Pfn1 sequence is listed above as it is the protein sequence utilized in all our assays. Each color represents the different types of amino acids conserved across species. The black bar graphs represent the consensus of the sequences. Residues circled in red represent locations of mutated residues relevant for actin, polyproline, or PIP2 binding. Residues circled in purple are important actin-binding residues. Created with Jalview.

The computational analysis and Matrigel cord formation assays performed by our collaborators, used mouse Pfn1, as the compounds were designed for evaluation in mouse models.

To keep our *in vitro* results comparable, our assays used mouse Pfn1. Pfn1 is known to be well conserved across evolution and therefore mouse Pfn1 serves as an appropriate surrogate for human Pfn1 in our models and assays (Figure 13). As integral actin-binding residues circled in purple (Figure 13) are very well conserved across evolution, mouse Pfn1 is a reasonable homolog to test compounds for future use in humans. Furthermore, the same can be said about polyproline binding, as the residue H133 is also well conserved and is known to play a critical role in mediating the Pfn1-polyproline binding interaction. Likewise, all four mutants that were developed to control and test for actin, proline, and PIP2 binding (H133S, R75E, R88L, and H119E) are in areas in the Pfn1 protein sequence that are well characterized and conserved across species.

3.3 3E-Pfn1 melting temperature shifts when proline peptide is added

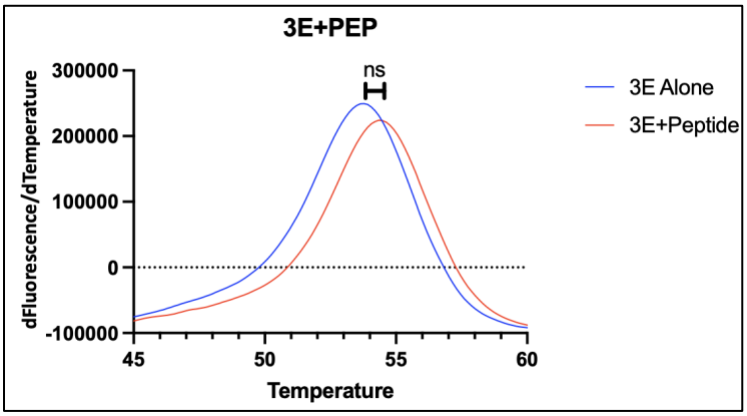

Figure 14. Protein Thermal Shift Assay of 3E-Pfn1 and peptide.

The addition of a polyproline peptide to 3E-Pfn1 causes an increase in melting temperature of 0.42° C, which is not statistically significant. The average melting temperature of 3E-Pfn1 alone is 53.73° C, while the average melting

temperature of 3E-Pfn1 with added peptide is 54.34° C. Each sample had three replicates and the data represent the average rate of change of fluorescence over the temperature gradient (p value = 0.10).

One of the steps necessary to prove that 3E-Pfn1 is functionally equivalent to WT-Pfn1 is confirmation that it binds like the WT-Pfn1. As Pfn1 is known to bind to proline sequences of 10-12 prolines at high affinity, I tested this binding with 3E-Pfn1 via a protein thermal shift (PTS) assay (PTS). PTS assays investigate melting temperatures of proteins to evaluate their stabilities. If 3E-Pfn1 is bound to a proline peptide sequence, its average melting temperature will be expected to change, conferring an observable shift in the melting temperatures between 3E-Pfn1 alone and 3E-Pfn1 with polyproline peptide.

PTS results showed an upward shift in melting temperature of 0.42 degrees when 3E-Pfn1 was bound to peptide, which presented a p-value of 0.10, which is not statistically significant (Figure 14). However, these results are promising and with further optimization could confer more definitive and statistically significant results. Additionally, it should be noted that the peptide was provided to us in a buffer containing Tris, which is not normally utilized in PTS assays due to its pH and not being thermostable. Even though I controlled for this in the 3E-Pfn1 alone sample by adding an equivalent concentration of Tris, future optimization of the assay should avoid using Tris in the buffer.

3.4 Crystallization

Another step I undertook in order to test whether 3E-Pfn1 could be a surrogate for wild-type Pfn1 in native PAGE assays, is to ensure that the addition of the 3E tag has not affected any part of the Pfn1 structure. This is especially important in areas like the actin binding site, in which changes could affect the result of the drug screening assays. To achieve this, X-ray crystallography will be used to determine the structure, because this structural technique yields the highest resolution data and is best suited for the relatively small size of 3E-Pfn1. There are three main steps in the process of determining the structure of a protein using X-ray crystallography. The first is the need to grow crystals of the 3E-Pfn1 protein. Conditions for the crystallization of WT-Pfn1 have been previously determined and provided the groundwork for establishing the crystallization conditions of 3E-Pfn1 (Zdancewicz, 2021). Following the growth of the crystals, diffraction data will need to be collected and processed to calculate an electron density map that can be used to build a model of the 3E-Pfn1.

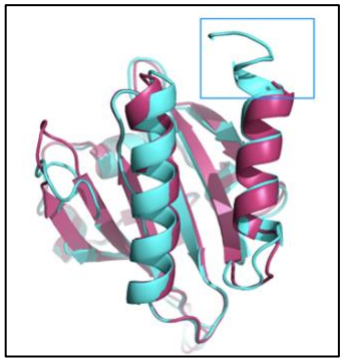

Figure 15. Hypothesized 3E-PFN1 structure.

WT-Pfn1 (Zdancewicz, 2021), (pink), overlayed with predicted 3E-Pfn1 structure (teal). Additional 3E residues are denoted in the blue box. The alignment has an RMSD of 0.751Å. Created with PyMOL.

After generating the model of the 3E-Pfn1 protein, it is necessary to compare it to WT-Pfn1 by aligning and overlaying the structures of both proteins using PyMOL (Figure 15). This comparison would identify any portions of the protein that differ between the two proteins. As a preliminary analysis that did not require any data collection, I generated a model of the 3E-Pfn1 structure using AlphaFold on the Pittsburgh Super Computing Center. I expected that if I saw any differences they would be localized at the N-terminus where the 3E tag has been added. Preliminary analysis has shown that the overlaid structure of WT-Pfn1 and 3E-Pfn1 has a root mean square deviation (RMSD) of 0.751Å (using all atoms), which validates that the structures are nearly identical. Confirming this was imperative to determine that wild-type WT-Pfn1 and 3E-Pfn1 are functionally equivalent, and that 3E-Pfn1 can be a surrogate for WT-Pfn1 on the native PAGE assay.

3.5 Conditions for crystallization of 3E-PFN1 are determined

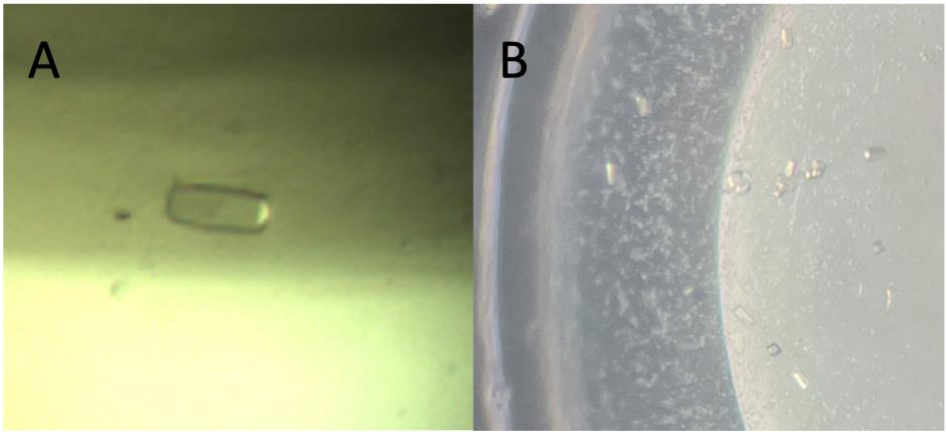

Figure 16. Crystallized WT-Pfn1 and 3E-Pfn1.

Crystals of (A) WT-Pfn1 (Zdancewicz, 2021) and (B) 3E-Pfn1 are shown. Both have similar crystallization conditions and similar crystal morphologies suggesting structural similarities and likely functional equivalence.

To confirm that 3E-Pfn1 is structurally and therefore functionally like WT-Pfn1, crystallization of 3E-Pfn1 is necessary. Starting with crystallization conditions determined by Sara Zdancewicz, I was able to crystallize 3E-Pfn1 and further optimize the conditions that work best for 3E-Pfn1. Those conditions produced crystals that were similar in morphology to those of the WT-Pfn1 (Figure 16). 3E-Pfn1 crystals grew best at pH 3.75 and 1.95M ammonium sulfate over the span of 10-14 days. Similarly, WT-Pfn1 crystallized at 1.65M ammonium sulfate with 100 mM pH 4 citric acid over the course of two weeks. In both cases, 3E-Pfn1 and WT-Pfn1 produced crystals that are orthorhombic in shape. Although it is not definitive, when crystals are similar in morphology it suggests that they are similar in structure or are at least packing in a similar manner. This suggests that the structure of 3E-Pfn1 is not likely to be significantly different from that of the WT protein.

4.0 Discussion and Future Directions

WT-Pfn1 is involved in many diverse cellular functions and is particularly involved in cytoskeletal dynamics with actin (Ding et al., 2012). Chiefly, Pfn1 modulates EC proliferation and motility in endothelial cells, which are central components of angiogenesis (Gau et al., 2018). This concept is important in attempting to modulate disruptive angiogenic processes like ocular angiogenesis in the eye and cancer proliferation generally (Qazi et al., 2009). Thus far, our collaborators have developed compounds specifically targeting WT-Pfn1 in order to disrupt pathologic ocular angiogenesis (Gau et al., 2018). Although there is still much to be understood about the interaction between Pfn1 and actin and how the compounds are disrupting this, my work lays the foundation for further experimental analysis with higher throughput.

Thus far, I was able to demonstrate that creating a new version of WT-Pfn1, 3E-Pfn1, can be run and visualized on native PAGE. This development opens the door for further compound screening and development at a more rapid pace. Likewise, all mutants of Pfn1 have been cloned into the "3E" vector, purified, and sequenced to confirm the presence of the correct codons for the additional three residues. Moving forward, it will be necessary to run all the mutants on native PAGE to confirm they are also able to run like 3E-Pfn1. However, my previous success with 3E-Pfn1 itself, suggests that the additional 3E mutants should also run on native PAGE because they have similar PIs.

Once it is confirmed that mutants in the 3E backbone can run on native PAGE, it will be necessary to utilize them as controls to ensure that 3E-Pfn1 is comparable to the WT. For example, it is expected that mutating the His133 to a serine will eliminate proline binding. This has been

proven in WT-Pfn1, and the same should be true with the three additional amino acids (Ding et al., 2009). Testing if 3E-Pfn1-H133S loses polyproline binding will be an experiment to perform. Furthermore, the mutants can be used to understand where the compounds bind to Pfn1, and if their binding is mediated by any other proteins like actin, proline motifs, or PIP2. This could be performed through compound titration assays on native PAGE to visualize the interaction, and to find a K_D to quantify the binding interaction between the compound and each of the four different mutants. PTS assays could also be used to obtain melting temperature shifts when compound is bound to WT-Pfn1, 3E-Pfn1, and see if this changes across the mutants. These assays would give us an indication of how tightly the compound is binding, and what mediators are necessary for binding. This information will be vital for further compound development.

Additionally, I want to repeat the PTS assay with 3E-Pfn1 and the polyproline peptide without Tris in either of the buffers. As stated previously, Tris should not be used in PTS assays because its pH is not thermostable and may have skewed the results. I intend to maintain the protein and peptide in a buffer with HEPES which will not impact the protein melting temperatures. This would allow me to ensure that the previous shift results I saw were true and allow me to hopefully obtain a statistically significant shift in melting temperature after binding.

Furthermore, I would like to continue trying to visualize 3E-Pfn1 binding to a polyproline sequence by fluorescence. Although the previous mechanism of cloning twelve prolines into the Clover vector was unsuccessful, our collaborators have a polyproline construct from the VASP protein, which when fluorescently tagged could be a sufficient binding control for 3E-Pfn1. In addition, I determined the best conditions to run the previous Clover construct under for sufficient visualization. This will make visualizing further iterations of the construct more straightforward. Likewise, Pfn1 binding to the proline motif on VASP has been well characterized with a known

K_D (Ferron et al., 2007). Through binding of 3E-Pfn1 with a fluorescently tagged VASP, I can calculate a K_D via native PAGE for 3E-Pfn1 and the VASP and compare it to the known value. The same can be performed on WT-Pfn1, as even though it will not run on native PAGE alone, as a complex with VASP, it can be visualized on native PAGE, and likewise have its K_D calculated. Therefore, a fluorescently tagged VASP will serve as a proper control mechanism for all versions of the Pfn1 protein utilized on native PAGE.

One of the concerns since binding was not present on previous iterations of the native PAGE assay between 3E-Pfn1 and a polyproline peptide is the possibility that 3E-Pfn1 was not fully folded. In literature from other groups that have purified Pfn1, it is often purified in the presence of VASP, allowing for only the fully folded and binding-functional protein, to be purified without its partially folded counterparts. This is a measure that I did not take when purifying Pfn1 variants. In the future to ensure that the purified Pfn1 that we are using is fully folded, we will test for molten globules or intermediate states of the protein via fluorescence anisotropy. Fluorescence anisotropy is able to differentiate between the unfolded, molten globule, and folded state of the protein (Canet et al., 2001). This allows us to confirm whether our purification methods are providing fully folded Pfn1 before we move forward with optimizing other components of our assays.

Considering the compound is computationally designed to bind Pfn1 and disrupt its interaction with actin, it will be important to ensure that the compound is specifically binding to Pfn1 and not binding or interacting with actin directly. It will be integral moving forward to test compound binding to actin. Actin, however, is biochemically difficult to purify, and to analyze its binding properly, it would have to be isolated in its ATP-bound, G-actin state. This however is difficult to do as the state of G-actin is unstable and it will tend to polymerize. To try to express a

version of actin that does not polymerize it will be necessary to do so within a eukaryotic expression system. My lab mate Sara Zdancewicz began attempting to express actin in the Expi293 cell line last semester, as that cell line is an iteration of HEK293s optimized for protein expression (Da Silva Junior, 2022). Her work was preliminary, and further optimization and effort by later lab members will be necessary for the successful purification of G-actin for future native PAGE and PTS assays.

References

Allen, A., Gau, D., Francoeur, P., Sturm, J., Wang, Y., Martin, R., Maranchie, J., Duensing, A., Kaczorowski, A., Duensing, S., Wu, L., Lotze, M. T., Koes, D., Storkus, W. J., & Roy, P. (2020). Actin-binding protein profilin1 promotes aggressiveness of clear-cell renal cell carcinoma cells. *J Biol Chem*, *295*(46), 15636-15649. https://doi.org/10.1074/jbc.RA120.013963

Brenton, A. G., & Godfrey, A. R. (2010). Accurate Mass Measurement: Terminology and Treatment of Data. *Journal of the American Society for Mass Spectrometry*, *21*(11), 1821-1835. https://doi.org/https://doi.org/10.1016/j.jasms.2010.06.006

Canet, D., Doering, K., Dobson, C. M., & Dupont, Y. (2001). High-Sensitivity Fluorescence Anisotropy Detection of Protein-Folding Events: Application to α-Lactalbumin. *Biophysical Journal*, *80*(4), 1996-2003. https://doi.org/https://doi.org/10.1016/S0006-3495(01)76169-3

Da Silva Junior, H. C. (2022). Transient Gene Expression in Human Expi293 Cells. In (pp. 319-325). Springer US. https://doi.org/10.1007/978-1-0716-1859-2_18

Ding, Z., Bae, Y. H., & Roy, P. (2012). Molecular insights on context-specific role of profilin-1 in cell migration. *Cell Adhesion & Migration*, *6*(5), 442-534. https://doi.org/10.4161/cam.21832

Ding, Z., Gau, D., Deasy, B., Wells, A., & Roy, P. (2009). Both actin and polyproline interactions of profilin-1 are required for migration, invasion and capillary morphogenesis of vascular endothelial cells. *Exp Cell Res*, *315*(17), 2963-2973. https://doi.org/10.1016/j.yexcr.2009.07.004

dos Remedios, C., Chhabra, D., Kekic, M., Dedova, I., Tsubakihara, M., Berry, D., & Nosworthy, N. J. (2003). Actin Binding Proteins: Regulation of Cytoskeletal Microfilaments. *Physiological reviews*, *83*, 433-473. https://doi.org/10.1152/physrev.00026.2002

Ezezika, O. C., Younger, N. S., Lu, J., Kaiser, D. A., Corbin, Z. A., Nolen, B. J., Kovar, D. R., & Pollard, T. D. (2009). Incompatibility with Formin Cdc12p Prevents Human Profilin from Substituting for Fission Yeast Profilin. *Journal of Biological Chemistry*, *284*(4), 2088-2097. https://doi.org/10.1074/jbc.m807073200

Ferron, F., Rebowski, G., Lee, S. H., & Dominguez, R. (2007). Structural basis for the recruitment of profilin–actin complexes during filament elongation by Ena/VASP. *The EMBO Journal*, *26*(21), 4597-4606. https://doi.org/10.1038/sj.emboj.7601874

Fierro, I. M. (2005). Angiogenesis and lipoxins. *Prostaglandins, Leukotrienes and Essential Fatty Acids*, *73*(3), 271-275. https://doi.org/https://doi.org/10.1016/j.plefa.2005.05.016

Fletcher, D. A., & Mullins, R. D. (2010). Cell mechanics and the cytoskeleton. *Nature*, *463*(7280), 485-492. https://doi.org/10.1038/nature08908

Gau, D., Lewis, T., McDermott, L., Wipf, P., Koes, D., & Roy, P. (2018). Structure-based virtual screening identifies a small-molecule inhibitor of the profilin 1-actin interaction. *J Biol Chem*, *293*(7), 2606-2616. https://doi.org/10.1074/jbc.M117.809137

Irwin, J. J., Sterling, T., Mysinger, M. M., Bolstad, E. S., & Coleman, R. G. (2012). ZINC: A Free Tool to Discover Chemistry for Biology. *Journal of Chemical Information and Modeling*, *52*(7), 1757-1768. https://doi.org/10.1021/ci3001277

Janmey, P. A., Bucki, R., & Radhakrishnan, R. (2018). Regulation of actin assembly by PI(4,5)P2 and other inositol phospholipids: An update on possible mechanisms. *Biochem Biophys Res Commun*, *506*(2), 307-314. https://doi.org/10.1016/j.bbrc.2018.07.155

Krüger, G., Blocki, Franke, & Jung. (2019). Vascular Endothelial Cell Biology: An Update. *International Journal of Molecular Sciences*, *20*(18), 4411. https://doi.org/10.3390/ijms20184411

Lu, J., & Pollard, T. D. (2001). Profilin Binding to Poly-<scp>l</scp>-Proline and Actin Monomers along with Ability to Catalyze Actin Nucleotide Exchange Is Required for Viability of Fission Yeast. *Molecular Biology of the Cell*, *12*(4), 1161-1175. https://doi.org/10.1091/mbc.12.4.1161

Qazi, Y., Maddula, S., & Ambati, B. K. (2009). Mediators of ocular angiogenesis. *Journal of Genetics*, *88*(4), 495-515. https://doi.org/https://doi.org/10.1007/s12041-009-0068-0

Rafii, S., Butler, J. M., & Ding, B.-S. (2016). Angiocrine functions of organ-specific endothelial cells. *Nature*, *529*(7586), 316-325. https://doi.org/10.1038/nature17040

Rao, J., & Li, N. (2004). Microfilament actin remodeling as a potential target for cancer drug development. *Curr Cancer Drug Targets*, *4*(4), 345-354. https://doi.org/10.2174/1568009043332998

Reinhard, M., Giehl, K., Abel, K., Haffner, C., Jarchau, T., Hoppe, V., Jockusch, B. M., & Walter, U. (1995). The proline-rich focal adhesion and microfilament protein VASP is a ligand for profilins. *Embo j*, *14*(8), 1583-1589. https://doi.org/10.1002/j.1460-2075.1995.tb07146.x

Skruber, K., Warp, P., Shklyarov, R., Thomas, J., Swanson, M., Henty-Ridilla, J., Read, T. A., & Vitriol, E. (2019). *Profilin 1 Controls the Assembly, Organization, and Dynamics of Leading Edge Actin Structures Through Internetwork Competition and Collaboration*. https://doi.org/10.1101/849356

Terman, J. R., & Kashina, A. (2013). Post-translational modification and regulation of actin. *Curr Opin Cell Biol*, *25*(1), 30-38. https://doi.org/10.1016/j.ceb.2012.10.009

Wagstaff, K. M., Dias, M. M., Alvisi, G., & Jans, D. A. (2005). Quantitative Analysis of Protein–Protein Interactions by Native Page/Fluorimaging. *Journal of Fluorescence*, *15*(4), 469-473. https://doi.org/10.1007/s10895-005-2819-5

Zdancewicz, S. (2021).